Journal of Solid State Chemistry 183 (2010) 702–706

Contents lists available at ScienceDirect

Journal of Solid State Chemistry

journal homepage: www.elsevier.com/locate/jssc

Synthesis and crystal structure of the isotypic rare earth thioborates Ce[BS_3], Pr[BS_3], and Nd[BS_3]

Jens Hunger, Marija Borna, Rüdiger Kniep *

Max Planck Institute for Chemical Physics of Solids, Nöthnitzer Strasse 40, D-01187 Dresden, Germany

ARTICLE INFO

Article history:
Received 29 October 2009
Received in revised form
24 December 2009
Accepted 3 January 2010
Dedicated to Professor Hans-Jörg Deiseroth on the occasion of his 65th birthday.
Available online 11 January 2010

Keywords:
Rare earth compounds
Thioborates
Preparation
Crystal structure

ABSTRACT

The orthothioborates Ce[BS_3], Pr[BS_3] and Nd[BS_3] were prepared from mixtures of the rare earth (*RE*) metals together with amorphous boron and sulfur summing up to the compositions CeB_3S_6, PrB_5S_9 and NdB_3S_6. The following preparation routes were used: solid state reactions with maximum temperatures of 1323 K and high-pressure high-temperature syntheses at 1173 K and 3 GPa. Pr[BS_3] and Nd[BS_3] were also obtained from rare earth chlorides $RECl_3$ and sodium thioborate $Na_2B_2S_5$ by metathesis type reactions at maximum temperatures of 1073 K. The crystal structure of the title compounds was determined from X-ray powder diffraction data. The thioborates are isotypic and crystallize in the orthorhombic spacegroup $Pna2_1$ (No. 33; $Z=4$; Ce: $a=7.60738(6)$ Å, $b=6.01720(4)$ Å, $c=8.93016(6)$ Å; Pr: $a=7.56223(4)$ Å, $b=6.00876(2)$ Å, $c=8.89747(4)$ Å; Nd: $a=7.49180(3)$ Å, $b=6.00823(2)$ Å, $c=8.86197(3)$ Å) . The crystal structures contain isolated $[BS_3]^{3-}$ groups with boron in trigonal-planar coordination. The sulfur atoms form the vertices of undulated kagome nets, which are stacked along [100] according to the sequence ABAB. Within these nets every second triangle is occupied by boron and the large hexagons are centered by rare earth ions, which are surrounded by overall nine sulfur species.

1. Introduction

Borates represent a well known class of compounds with a wide range of applications. Especially in the field of optical materials, *RE* oxoborates play a major role. Although a huge number of crystal structures of oxoborates is known, the crystal chemistry of thioborates is less investigated. Thus, we started to prepare thioborates of the rare earth metals, where the driving idea behind was the preparation of low-dimensional materials which might have interesting (*RE*-dominated) physical properties. So far, there is only one report on a crystal structure of a *RE* thioborate (Eu[B_2S_4] [1]). Obviously, this is mainly due to the lack of improved preparation techniques for thioborate syntheses. Therefore, we started to develop and optimize useful preparation routes.

Binary boron sulfides as well as ternary and quaternary thioborates contain boron in trigonal-planar and/or tetrahedral coordination, forming various types of chalcogenoborate complexes [2]. Small, highly charged ions such as $[BS_3]^{3-}$ [3–5], $[B_2S_4]^{2-}$ [6], $[B_2S_5]^{2-}$ [7], and $[B_3S_6]^{3-}$ [5,8–10] are typical for systems with trigonal-planar coordinated boron. Structures with boron in tetrahedral coordination tend to form larger complex anions [11–14].

Here, we report on different preparation routes and describe the crystal structures of *RE*[BS_3] (*RE* = Ce, Pr, Nd) as first examples of ternary thioborates containing trivalent cations. The synthesis of *RE* thio- and selenoborates from the elements (and/or binary compounds) is fairly problematic because of the high reactivity of the *in situ* formed boron chalcogenides towards most of the common container materials at elevated temperatures. Silica glass tubes are attacked by boron chalcogenides at temperatures above 700 K (B/Si exchange). Carbon-coated silica tubes, often used for the synthesis of alkali and alkaline earth chalcogenoborates, are disadvantageous with respect to longer reaction times and temperatures above 1200 K. For such kind of reactions the vessels must be made of either boron nitride or glassy carbon. The chalcogenoborates of the heavier chalcogens are sensitive against oxidation and moisture and, hence, they have to be handled in an inert environment.

It is well known that *RE* polychalcogenides [15] and nitridoborates [16] can be obtained by metathesis reactions at moderate temperatures. Employing this method we carried out similar experiments for the preparation of *RE* thioborates [17] which indeed appeared to be a promising route.

2. Materials and methods

Our attempts to optimize the high-temperature routes (beyond the melting points of the *RE* metals) led to the

* Corresponding author.
E-mail address: kniep@cpfs.mpg.de (R. Kniep).

0022-4596/$ - see front matter © 2010 Elsevier Inc. All rights reserved.
doi:10.1016/j.jssc.2010.01.002

development of specially designed crucibles made of sintered boron nitride (without any binder component) enclosed in tantalum ampoules. These ampoules were placed in quartz glass reactors under flowing argon and heated in a tube furnace. Nevertheless, this equipment has still some disadvantages caused by the reaction of the boron chalcogenide gas phase with tantalum at temperatures above 1200 K. However, a stable, protective layer of tantalum sulfide that prevents further reaction of the sample with the ampoule material can be generated by means of excess boron and chalcogen in the reaction mixture. For the time being, the maximum temperature of this equipment is limited to 1450 K. The development of closed (pressure-resistant) boron nitride lined reactors operating at even higher temperatures is in progress.

For evaluation purposes we reinvestigated the only known *RE* thioborate, EuB_2S_4 [1], which is an isotype of SrB_2S_4 [18]. Starting from the elements, the syntheses were successful, and the purity of the reaction products was higher than the values reported for the samples originally prepared in carbon-coated quartz glass ampoules. Attempts to grow single crystals by chemical transport reaction with iodine failed so far. Subsequently, the ternary systems Ce–B–S, Nd–B–S and Pr–B–S were investigated. At temperatures below the melting points of the respective *RE* metals, only binary phases are formed as the major components together with small amounts of unknown phases (depending on the composition, sample loading, and temperature). At temperatures above 1323 K and with high sample loadings nearly single phase products of $Pr[BS_3]$ and $Nd[BS_3]$ as well as $Ce[BS_3]$ contaminated with small amounts ($\approx 8\%$) of CeS_2, were obtained. Furthermore, $Pr[BS_3]$ and $Nd[BS_3]$ were prepared by application of external pressure (3 GPa, 1173 K, 30 min) by means of a multianvil press as described in [19] and by metathesis type reactions, respectively.

The reaction products were characterized by means of X-ray powder diffraction, scanning electron-microscopy and energy-dispersive X-ray spectroscopy (EDXS).

2.1. Materials

For the preparations from the elements neodymium (powder, ChemPur, 99.9%), praseodymium (powder, ChemPur, 99.9%), cerium (chips, ChemPur, 99.9%) and amorphous boron (powder, ABCR, 99%) were used as purchased without further purification. Sulfur (Alfa Aesar, 99.9995%) was sublimed under vacuum to reduce oxygen contamination below 1%. $Na_2B_2S_5$, used for metathesis reactions, was prepared from Na_2S (Strem, 95%), amorphous boron and sulfur according to literature data [7]. $NdCl_3$ (Aldrich, 99.99%) and $PrCl_3$ (Aldrich, 99.99%) were used without any further purification. All educts were checked by means of elemental analysis using a LECO RH 404 analyzer (H), LECO TC 436 DR/5 analyzer (N/O), LECO C-200 CHLH analyzer (C) and a simultanious inductively coupled plasma-optical emission (ICP-OES) Echelle spectrometer (other elements), respectively.

2.2. Syntheses

2.2.1. High-temperature routes

Mixtures of rare earth metal powders, amorphous boron and sulfur were ground, cold pressed and again ground. Due to the side reaction of B_2S_3 with tantalum some excess boron and sulfur were used. By this, the educts sum up to the total compositions CeB_3S_6, PrB_5S_9 and NdB_3S_6, respectively. Molar ratios corresponding to the compositions $CeBS_3$, CeB_2S_5, CeB_4S_8, CeB_5S_9, $PrBS_3$, PrB_3S_6, $NdBS_3$ and NdB_5S_9 did not yield sufficiently pure reaction products. The resulting powders were filled in boron nitride crucibles (diameter 16/10 mm, height 50 mm), which were deposited in sealed tantalum ampoules (diameter 18 mm) under ambient argon pressure. The complete reaction containers were deposited in quartz reactors with connections to argon supply and relief pressure valve and tempered using an one-zone vertical tube furnace. The reactions were carried out under constant argon flow by applying the following temperature program: $298\,K \xrightarrow{5\,h} 673\,K(5\,h) \xrightarrow{10\,h} 1023\,K(10\,h) \xrightarrow{20\,h} 1323\,K(300\,h) \xrightarrow{150\,h} 473\,K \xrightarrow{5\,h} 298\,K$.

2.2.2. High-pressure high-temperature routes

Pressure transmission was realized by octahedra made of MgO with an edge length of 18 mm. Reaction temperatures were adjusted by resistance heating using graphite tubes. Pressure and temperature calibration was performed prior to the experiments by *in situ* monitoring of the resistance changes of elemental bismuth and by performing runs using a thermocouple. Hexagonal boron nitride was used as the crucible material. The syntheses were accomplished at 1173 K and 3 GPa for 30 min. No indications of reactions between the container material and the sample were observed, and the reaction products could easily be removed from the crucibles.

2.2.3. Metathesis reactions

Our first attempts in running metathesis reactions in carbon crucibles inserted in silica ampoules revealed that significant reactions between the container material and gaseous B-S species take place yielding in quaternary sulfides, such as $RE_9AlSi_3S_{21}$. Therefore, tantalum was used instead of silica. $RE[BS_3]$ was obtained from mixtures of $Na_2B_2S_5$ [7] and $RECl_3$ in the molar ratio 3:2. The reactions were carried out in an one-zone vertical tube furnace by applying the following temperature program: $298\,K \xrightarrow{8\,h} 1073\,K(16\,h) \xrightarrow{60\,h} 298\,K$. Subsequent separation of the reaction products ($RE[BS_3]$ and NaCl) by sublimation at

Table 1
Crystallographic data of the isotypic phases $RE[BS_3]$ (RE = Ce, Pr, Nd). See also Table S1 in the supporting information.

	$Ce[BS_3]$	$Pr[BS_3]$	$Nd[BS_3]$
Color	Yellow-green	Emerald green	Light green
Space group, Z	$Pna2_1$, 4	$Pna2_1$, 4	$Pna2_1$, 4
Formula mass [g mol^{-1}]	247.11	247.90	251.23
Radiation, λ [Å]	Cu Kα_1, 1.540562	Cu Kα_1, 1.540562	Cu Kα_1, 1.540562
Temperature [K]	298	298	298
Diffractometer	G670	G670	G670
a [Å]	7.60873(4)	7.55960(5)	7.48692(3)
b [Å]	6.01685(2)	6.00673(3)	6.00551(2)
c [Å]	8.93188(4)	8.89435(5)	8.85815(3)
Cell volume [Å^3]	408.906(3)	403.879(4)	398.287(2)
Density [g cm^{-3}]	4.014	4.077	4.190
Weighted profile R-factor R_{wp}	0.023	0.044	0.022
Profile R-factor R_p	0.015	0.028	0.016
Structure R-factor R_F	0.051	0.098	0.056
Expected R-factor R_{exp}	0.019	0.017	0.018

Rietveld refinement was used to minimize $\sum w_i(I_{o,i}-I_{c,i})^2$ where $I_{o,i}$ and $I_{c,i}$ are the observed and calculated powder diffraction intensities for the i th point, respectively. Weights, w_i, are $1/I_{o,i}$. Weighted and unweighted profile R-factors are defined as $R_{wp} = \sqrt{\sum w_i(I_{o,i}-I_{c,i})^2 / \sum w_i(I_{o,i})^2}$ and $R_p = \sum |(I_{o,i}-I_{c,i})| / \sum I_{o,i}$. The structure factor R_F is defined as $R_F = \sum(F_o-F_c)^2 / \sum(F_o)^2$. The expected R-factor (the statistically best possible value for R_{wp}) is defined as $R_{exp} = \sqrt{N-P / \sum w_i(I_{o,i})^2}$ where N is the number of observed powder diffraction data points and P is the number of refined parameters.

temperatures between 973 and 1173 K in carbon crucibles enclosed in fused silica ampoules was not satisfactory and led to decomposition of *RE*[BS_3] to some unidentified phases. However, separation of the reaction products was successfully accomplished by application of a temperature gradient at the beginning of the cooling step by vertical shifting of the tantalum ampoule with its top looking out of the furnace.

2.3. X-ray diffraction

The crystal structures of *RE*[BS_3] (*RE* = Ce, Pr, Nd) were solved from X-ray powder diffraction data (298 K, flat-plate samples on a Huber G670 Guinier-Camera with Cu Kα_1 radiation in the angular range $2\theta = 3-100^\circ$ as well as samples in a capillary on a STOE StadiP-MP diffractometer using Debye-Scherrer geometry with Mo Kα_1 radiation in the angular range $2\theta = 2-100^\circ$, both equipped with a Ge monochromator) by Monte Carlo indexing [20] and direct space structure solution methods [21]. The crystal structures were found to be isotypic (Tables 1 and S1 in the supporting information).

Subsequently, the Rietveld refinement method [22] was applied by using the GSAS software package [23,24] (Fig. 1 and Figs. S1–S4 in the supporting information). The position of the boron atoms was restrained near the center of gravity of the sulfur atoms of the [BS_3] units. The isotropic displacement parameters of the sulfur atoms were constrained to be equal and the corresponding parameter of the boron site was constrained to be 1.5 times that of the attached sulfur atoms. Alternatively the derivative difference minimization method was used [25]. The differences in the results of the two different types of structure refinements allow some rough estimation of the real uncertainties of the structural parameters, which are expected to be about two orders of magnitude higher than the standard deviations obtained by the Rietveld refinements. Nevertheless, the latter values will be used in the following. For determination of more reliable values for the lattice constants diffraction data obtained from mixtures of *RE*[BS_3] and LaB_6 (NIST SRM 660a, $a = 4.156916(10)$ Å) as internal standard were fitted without use of any structural model (Le Bail fit).

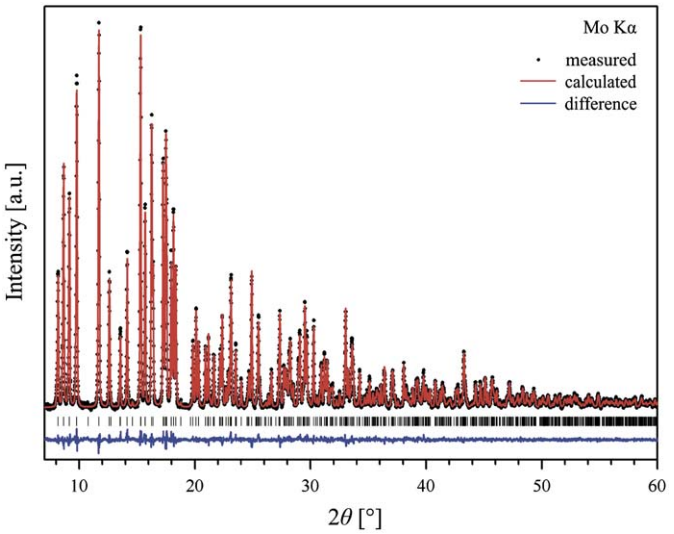

Fig. 1. X-ray powder diffraction pattern and Rietveld refinement of Pr[BS_3].

2.4. Scanning electron microscopy and EDXS

Scanning electron microscopy (Fig. 2) and the determination of the chemical composition of the bulk samples by energy dispersive X-ray spectroscopy (EDXS) were performed by use of a SEM Philips XL 30 with integrated energy dispersive spectrometer.

In agreement with the results of the crystal structure determinations EDXS confirmed the presence of boron and the molar ratios *RE*:S of 1:3.

3. Results and discussion

RE[BS_3] is only formed with sample loadings larger than 0.12 grams per cubic centimeter of the free ampoule volume and at temperatures above 1323 K. Obviously, a significant pressure of B_2S_3 and/or the melt of the *RE* metal are needed for the reaction from the elements. At lower temperatures the binary sulfides are obtained as the reaction products. For the preparation of *RE*[BS_3] also excess boron and sulfur in the reaction mixtures are needed. Best results were obtained with mixtures of educts summing up to the compositions CeB_3S_6, PrB_5S_9 and NdB_3S_6. Attempts to grow single crystals of *RE*[BS_3] by long-time annealing or by chemical transport reaction were not successful. Only large single crystals of α-Nd_2S_3 with a new three-dimensional superstructure were grown by the transport reactions. Metathesis reactions of lithium thioborate $Li_2B_2S_5$ [7] with *RE*Cl_3 did not result in the desired orthothioborates. The thioborates *RE*[BS_3] are only obtained by metathesis reactions with $Na_2B_2S_5$ [7].

In the crystal structure of *RE*[BS_3] (*RE* = Ce, Pr, Nd) (orthorhombic, $Pna2_1$, No. 33; $Z = 4$) the atoms exclusively occupy general positions (Table 2). The sulfur atoms form the vertices of

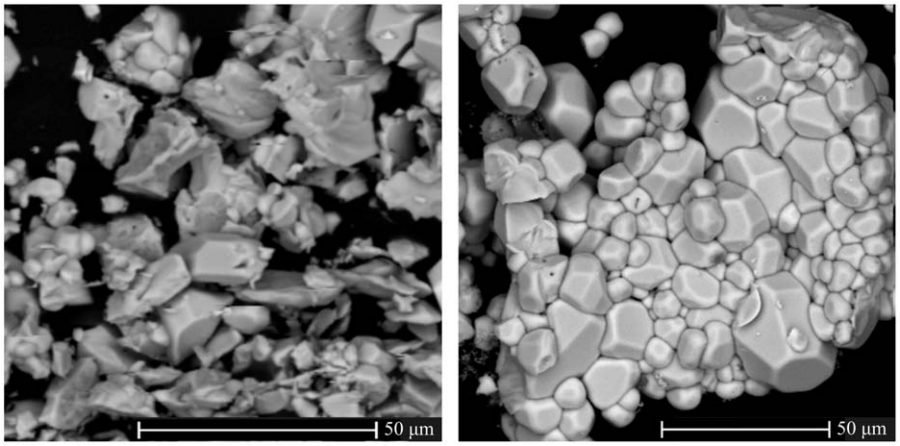

Fig. 2. BSE images of microcrystalline Pr[BS_3] (left) and Nd[BS_3] (right).

Table 2
RE[BS_3] (*RE* = Ce, Nd, Pr): Fractional atomic coordinates and isotropic displacement parameters; estimated standard deviations are given in parentheses.

Atom	Site	*x*	*y*	*z*	U_{iso} [Å^2]
Ce[BS_3]					
Ce1	4a	0.88549(6)	0.57017(7)	0.7547(3)	0.00958(9)
B1	4a	0.3427(2)	0.4183(2)	0.92973(15)	0.0190(5) [a]
S1	4a	1.00058(17)	0.8964(3)	0.27162(15)	0.0127(3) [a]
S2	4a	0.2016(3)	0.6670(2)	0.54280(18)	0.0127(3) [a]
S3	4a	0.3252(2)	0.1363(3)	0.46043(17)	0.0127(3) [a]
Pr[BS_3]					
Pr1	4a	0.88487(8)	0.56806(10)	0.7474(4)	0.00783(17)
B1	4a	0.3503(4)	0.4162(4)	0.9301(3)	0.0159(9) [a]
S1	4a	0.9911(3)	0.8908(5)	0.2714(2)	0.0106(6) [a]
S2	4a	0.2011(5)	0.6664(4)	0.5435(3)	0.0106(6) [a]
S3	4a	0.3179(4)	0.1366(4)	0.4563(3)	0.0106(6)[a]
Nd[BS_3]					
Nd1	4a	0.88425(5)	0.56774(6)	0.7550(4)	0.00694(8)
B1	4a	0.3494(12)	0.3898(13)	0.9189(3)	0.0133(7) [a]
S1	4a	0.99474(19)	0.8966(3)	0.2705(2)	0.0089(3) [a]
S2	4a	0.1796(3)	0.6674(4)	0.55601(18)	0.0089(3) [a]
S3	4a	0.2943(3)	0.1329(4)	0.46569(17)	0.0089(3) [a]

[a] The isotropic displacement parameters of the sulfur atoms were constrained to be equal and the corresponding parameter of the boron site was constrained to be 1.5 times that of the attached sulfur atoms.

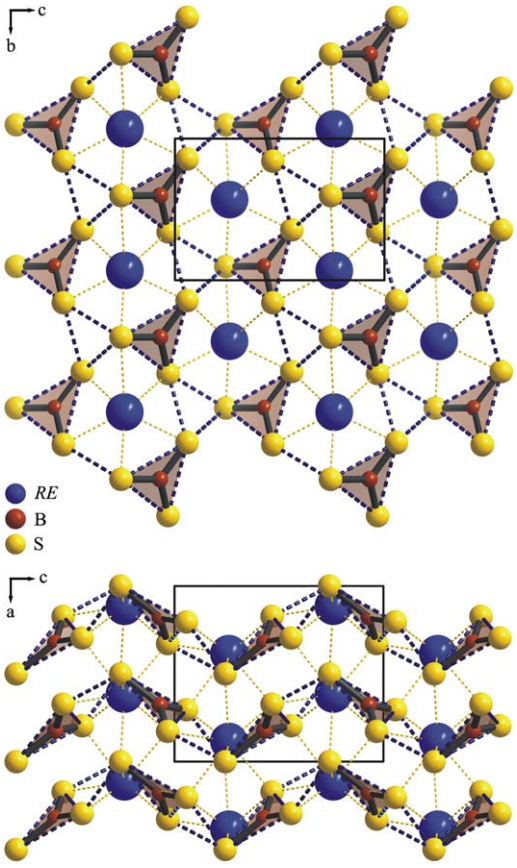

Fig. 3. Crystal structure of *RE*[BS_3] (*RE* = Ce, Pr, Nd) viewed along [100] (top) and [010] (bottom). The corrugated kagome nets formed by the S atoms are sketched with blue dotted lines.

corrugated kagome nets (Fig. 3). Within these nets every second triangle is occupied by boron and the large hexagons are centered by *RE* cations. The layers are stacked along [100] according to the sequence ABAB. The *RE* cations are surrounded by nine sulfur

Table 3
Interatomic distances (Å) within the coordination polyhedra around *RE* cations and bond lengths and angles (°) within the $[BS_3]^{3-}$ units in the crystal structures of *RE*[BS_3] (*RE* = Ce, Pr, Nd). See also Fig. S5 in the supporting information.

Ce[BS_3]		Pr[BS_3]		Nd[BS_3]	
Atoms	Distance	Atoms	Distance	Atoms	Distance
Ce1–S2	2.835(3)	Pr1–S2	2.787(5)	Nd1–S2	2.826(3)
Ce1–S3	2.895(3)	Pr1–S3	2.911(5)	Nd1–S2	2.890(3)
Ce1–S1	2.942(2)	Pr1–S1	2.919(3)	Nd1–S3	2.911(4)
Ce1–S3	2.943(3)	Pr1–S3	2.945(4)	Nd1–S3	2.916(3)
Ce1–S3	3.011(2)	Pr1–S3	2.991(4)	Nd1–S1	2.935(2)
Ce1–S2	3.016(3)	Pr1–S1	3.043(2)	Nd1–S1	3.021(2)
Ce1–S2	3.115(3)	Pr1–S2	3.056(5)	Nd1–S2	3.055(4)
Ce1–S1	3.122(2)	Pr1–S2	3.058(5)	Nd1–S3	3.070(3)
Ce1–S1	3.328(2)	Pr1–S1	3.390(3)	Nd1–S1	3.345(2)
B1–S2	1.849(2)	B1–S2	1.849(3)	B1–S2	1.818(6)
B1–S3	1.852(2)	B1–S3	1.851(3)	B1–S3	1.861(8)
B1–S1	1.853(2)	B1–S1	1.858(3)	B1–S1	1.758(6)
Atoms	Angle	Atoms	Angle	Atoms	Angle
S2–B1–S3	111.88(11)	S2–B1–S3	111.55(19)	S2–B1–S3	111.0(3)
S1–B1–S2	118.38(11)	S1–B1–S2	118.90(17)	S1–B1–S2	126.6(5)
S1–B1–S3	127.39(10)	S1–B1–S3	126.72(17)	S1–B1–S3	122.2(4)

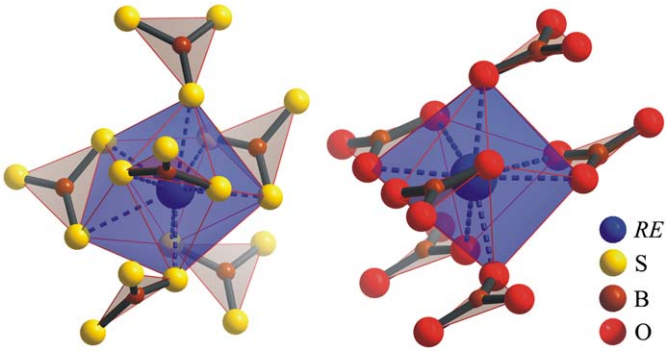

Fig. 4. Coordination environment of *RE* cations in the crystal structures of *RE*[BS_3] (left) and the isotypic phases o-Ce[BO_3] [27] and λ-Nd[BO_3] [26] (right).

species (Table 3) originating from six neighboring thioborate units (Fig. 4). Three of these units act as bidentate ligands whereas the remaining three $[BS_3]^{3-}$ groups are in a monodentate function.

Bond lengths and angles within the planar thioborate units are similar to the values observed in related compounds of alkali and alkaline earth metals. Overall, the $[BS_3]^{3-}$ groups in the crystal structures of *RE*[BS_3] are more distorted. This is assumed to be aroused by the higher charge of the cations and the decrease of the cation/anion ratio. The thioborate units are surrounded by six *RE* cations, three from the same kagome net and three from the two neighboring nets. This situation reflects the significant difference to the crystal structures of λ-Nd[BO_3] (Aragonite type) [26] and the isotypic o-Ce[BO_3] [27] where the three out-of-net *RE* ions contributing to the coordination sphere of the $[BX_3]^{3-}$ units come from one neighboring layer only (Fig. 5).

4. Conclusions

After development of various preparation routes we succeeded in the synthesis of the isotypic RE^{3+} orthothioborates, Ce[BS_3], Pr[BS_3] and Nd[BS_3]. Their crystal structure was solved and refined from X-ray powder diffraction data. The structural features of the isotypic phases show great similarities to those

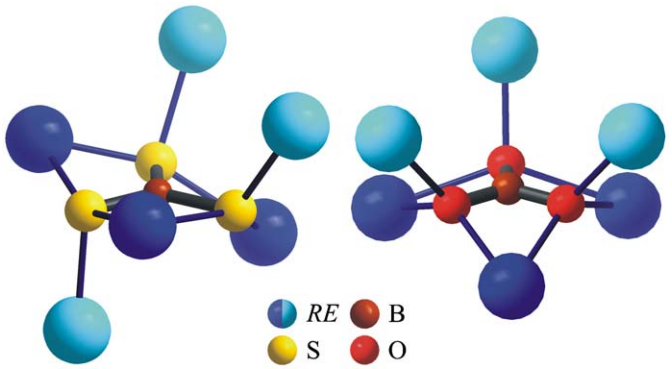

Fig. 5. Comparison of the environments of the $[BS_3]^{3-}$ unit in $RE[BS_3]$ (RE = Ce, Nd, Pr) (left) with the coordination of $[BO_3]^{3-}$ in λ-Nd$[BO_3]$ and o-Ce$[BO_3]$, respectively (right). *RE* cations from the same and the neighboring kagome nets are shown in dark blue and light blue, respectively.

of oxoborates $RE[BO_3]$ and orthothioborates of alkali and akaline earth metals. Besides the more conventional high-temperature route, metathesis reactions as well as high-pressure high-temperature reactions appear to be promising routes for the preparation of rare earth thioborates. Moreover, these reactions may open the way for the preparation of *RE* selenoborates after optimization of the reaction conditions.

Acknowledgments

We would like to thank Ulrich Burkhardt and Petra Scheppan (EDXS), Horst Borrmann, Steffen Hückmann and Jörg Lincke (X-ray powder diffraction), Gudrun Auffermann and Anja Völzke (elemental analysis) as well as Susann Leipe for her help with high-pressure high-temperature techniques. The authors are grateful to Bernt Krebs and Adrienne Hammerschmidt for fruitful discussions.

Supplementary data

Further details of the crystal structure investigations may be obtained from Fachinformationszentrum Karlsruhe, 76344 Eggenstein-Leopoldshafen, Germany (fax: (+49)7247-808-666; e-mail: crysdata@fiz-karlsruhe.de, http://www.fiz-karlsruhe.de/request_for_deposited_data.html) on quoting the CSD numbers 421071-421073. Rietveld plots and additional figures as well as CIF files of the title compounds are presented in the supporting information.

Appendix A. Supporting information

Supplementary data associated with this article can be found in the online version at doi:10.1016/j.jssc.2010.01.002.

References

[1] M. Döch, A. Hammerschmidt, B. Krebs, Z. Anorg. Allg. Chem. 630 (4) (2004) 519–522.
[2] O. Conrad, C. Jansen, B. Krebs, Angew. Chem., Int. Ed. 37 (2) (1998) 3209–3218.
[3] P. Vinatier, P. Gravereau, M. Menetrier, L. Trut, A. Levasseur, Acta Crystallogr., Sect. C: Cryst. Struct. Commun. C 50 (8) (1994) 1180–1183.
[4] F. Hiltmann, C. Jansen, B. Krebs, Z. Anorg. Allg. Chem. 622 (9) (1996) 1508–1514.
[5] F. Hiltmann, B. Krebs, Z. Anorg. Allg. Chem. 621 (3) (1995) 424–430.
[6] A. Hammerschmidt, C. Jansen, J. Küper, C. Püttmann, B. Krebs, Z. Anorg. Allg. Chem. 621 (8) (1995) 1330–1337.
[7] C. Jansen, J. Küper, B. Krebs, Z. Anorg. Allg. Chem. 621 (8) (1995) 1322–1329.
[8] F. Chopin, A. Hardy, Compt. Rend. 261 (1(Groupe 8)) (1965) 142–144.
[9] C. Püttmann, H. Diercks, B. Krebs, Phosphorus, Sulfur, and Silicon and the Related Elements 65 (1) (1992) 1–4.
[10] F. Chopin, G. Turrel, J. Mol. Struct. 3 (1–2) (1969) 57–65.
[11] F. Hiltmann, P. zum Hebel, A. Hammerschmidt, B. Krebs, Z. Anorg. Allg. Chem. 619 (2) (1993) 293–302.
[12] B. Krebs, H. Diercks, Z. Anorg. Allg. Chem. 518 (1984) 101–114.
[13] A. Hammerschmidt, P. Hebel, F. Hiltmann, B. Krebs, Z. Anorg. Allg. Chem. 622 (1) (1996) 76–84.
[14] T. Kajiki, Y. Hayashi, H. Takizawa, Mater. Lett. 61 (11–12) (2007) 2382–2384.
[15] J.H. Chen, P.K. Dorhout, J. Solid State Chem. 117 (2) (1995) 318–322.
[16] H. Jing, B. Blaschkowski, H.-J. Meyer, Z. Anorg. Allg. Chem. 628 (9–10) (2002) 1955–1958.
[17] J.B. Wiley, R.B. Kaner, Science 255 (5048) (1992) 1093–1097.
[18] C. Püttmann, W. Hamann, B. Krebs, Eur. J. Inorg. Chem. 29 (4–5) (1992) 857–872.
[19] A. Wosylus, Y. Prots, U. Burkhardt, W. Schnelle, U. Schwarz, STAM 8 (5) (2007) 383–388.
[20] A.L. Bail, Powder Diffr. 19 (3) (2004) 249–254.
[21] V. Favre-Nicolin, R. Černý, J. Appl. Crystallogr. 35 (6) (2002) 734–743.
[22] H.M. Rietveld, J. Appl. Crystallogr. 2 (2) (1969) 65–71.
[23] A. Larson, R.V. Dreele, General structure analysis system (gsas), Los Alamos National Laboratory Report LAUR 86-748.
[24] B.H. Toby, J. Appl. Crystallogr. 34 (2) (2001) 210–213.
[25] L.A. Solovyov, J. Appl. Crystallogr. 37 (5) (2004) 743–749.
[26] H. Müller-Bunz, T. Nikelski, T. Schleid, Z. Naturforsch. 58b (2003) 375–380.
[27] F. Goubin, Y. Montardi, P. Deniard, X. Rocquefelte, R. Brec, S. Jobic, J. Solid State Chem. 177 (1) (2004) 89–100.